*Fine Structure and Dynamics of the Solar Atmosphere*
*Proceedings IAU Symposium No. 327, 2016*
*S. Vargas Domínguez, A.G. Kosovichev, P. Antolin & L. Harra, eds.*

doi:10.1017/S1743921317000138

# Small magnetic structures near the polar regions of the Sun

**I. Cabello**[1], **J. Blanco Rodríguez**[2], **L. Balmaceda**[3] **and V. Domingo**[2]

[1]UTN-Facultad Regional Mendoza, CONICET, CEDS, Mendoza, Argentina
email: icabello@mendoza-conicet.gob.ar

[2]Grupo de Astronomía y Ciencias del Espacio/Image Processing Laboratory, Universitat de València, Spain

[3]George Mason University, Fairfax, VA, USA

**Abstract.** The study of the small magnetic structures of the solar photosphere is of great relevance because of their association with concentrations of magnetic field and their possible contribution to the variations of the Total Solar Irradiance. These structures are known to appear close to active regions and ubiquitously in the quiet Sun areas. Numerous studies about their distribution across all over the solar surface have been done with high-resolution instrumentation. However, since the observations have always been carried out from the ecliptic plane, their distribution near the polar regions is not well known. Future missions, like Solar Orbiter, will certainly provide valuable information on these yet unexplored regions. In this work, and in preparation for that moment, we select favorable periods for the observation of the polar regions of the Sun, and study the fraction of covered surface by small magnetic structures and its variation with the solar activity.

**Keywords.** Sun: photosphere, Sun: magnetic fields, Sun: activity

## 1. Introduction and motivation

In the solar photosphere a wide range of magnetic structures are observed, mainly differing in their size and intensity contrast. Large structures as sunspots and pores are well known. The smallest ones are the Bright Points (BPs) and their contribution to the overall magnetic field and to the variations of the Total Solar Irradiance (TSI) is not yet well known. Knowing their distribution over the solar disk helps us to gain insight on these issue. BPs are known to appear everywhere, not only close to active regions (AR), but also in the quiet Sun (QS), in the border of the network as well as within the internetwork. However, since the observations have been always carried out from the ecliptic plane, how the concentration of BPs varies when approaching the poles is not well known.

The Solar Orbiter mission will be launched on 2018 and will observe the Sun from angles up to 30° outside the ecliptic, allowing us to observe the polar regions of the Sun. Nowadays, a preliminary study is possible because the terrestrial views of the Sun on March and September show the rotation axis tilted 7.25° with respect to the ecliptic plane, in such a way that the South pole can be observed on March and the North pole on September. In Bonet *et al.* (2012), the Center-to-Limb Variation (CLV) of the Fraction of Covered Surface (FCS) of BPs from the solar disk center to the South limb was analyzed with SST data. BPs were selected by an interactive tool which allows the user to choose the structures one by one.

In this work the CLV of the FCS of BPs is analized from a large data set corresponding to March and September from 2007 to 2015 along the central meridian of the Sun.

## 2. Data

A sequence of G-band images from the Solar Optical Telescope (SOT) on board Hinode (Kosugi *et al.*, 2007) have been selected. The selected data cover observations along the solar central meridian on March and September from 2007 until 2015. G-band images are obtained from a 8 Å wide filter centered at 4305.0 Å of the CH I line and have a spatial sampling of 0.0541 arcsec pixel$^{-1}$ and a 2×2 binning, resulting therefore in 0.1082 arcsec pixel$^{-1}$. The standard corrections of flat-field, dark current and cosmic rays were applied. In addition, the limb darkening effect has also been corrected and the sky background has been removed in images close to the limb.

## 3. Observation and selection of structures

Visual inspection shows that BPs at the solar disk center are easily observable because they are bright and have a circular shape, but towards the limb they appear more flattened and their observation becomes more difficult. Despite the magnetic nature of features under study, magnetograms were not used to select structures. While some authors (e.g. Blanco Rodríguez *et al.*, 2007; Domingo *et al.*, 2005) have used magnetograms to detect small magnetic structures like faculae, selection of structures with smaller spatial scales and fast temporal evolution, i.e. BPs, is difficult because magnetograms do not have the required sensitivity (Berger & Title, 2001). G-band images are considered as the best indicators to observe small magnetic structures in the photosphere, allowing very short exposure times.

For the selection of structures in this work, three different techniques were considered: an interactive selection tool, an intensity threshold selection criteria and a semi-interactive selection tool. The interactive selection tool was used in the work of Bonet *et al.* (2012), in the same way to that described by Sánchez Almeida *et al.* (2010). With this tool, the structures are selected one by one observing their evolution via the analysis of a time series. It is an excellent way to detect BPs but it is not convenient with a large amount of data. Defining an intensity threshold allows to have an estimation of the BPs. However, it does not only select BPs, but also bright pixels corresponding to other structures, such as granules, while some BPs not too bright are not taken. Finally, the semi-interactive tool works with a set of parameters like the image scale, the BPs size and others related to the intensity. It requires to do some tests to choose the optimum set of parameters that can offer a good selection of BPs. For the present work, results from the intensity threshold criteria and from the semi-interactive tool are compared.

### 3.1. *Threshold selection criteria*

An intensity threshold has been defined in order to select structures according to their brightness level, so those pixels with an intensity higher than this threshold level are selected. The threshold level, chosen after careful visual consideration, was defined as 1.3 times the medium intensity of each image.

### 3.2. *Semi-interactive selection tool*

As an alternative way for the structure selection for this study, a semi-interactive tool developed by Bovelet & Wiehr (2007) was applied. The selection of structures with this so-called MLT_4 (Multiple-Level Pattern Recognition) algorithm is based in intensity, similar to the selection in Section 3.1 but, unlike the threshold criteria, this tool splits the image in features and the selection is done for whole structures, not just individual pixels. To this end, the algorithm performs a pattern of recognized features in the input image, following 4 phases of treatment: (1) segmentation at equidistant levels from maximum

https://doi.org/10.1017/S1743921317000138 Published online by Cambridge University Press

to zero intensity, yielding a pattern of cells surrounding each local intensity maximum, (2) normalization of the pixel intensities of each cell from the previous step to their maximum value, (3) merging of over-segmented cells that result from the phase 1, and (4) shrinking of the normalized cells to reasonable sizes in accordance with their photometric appearance in the original image.

This algorithm analyzes images in byte format and takes as input parameters the image scale and preferences of the work mode (i.e. analyzing full image at once or by boxes, and excluding or including features at the boxes edges). In addition, intensity values and number of pixels required for each of the 4 phases, as well as maximum size of the intergranular lanes and minimum size of the features are specified. This tool can be considered as an interactive tool because some of the input parameters (byte levels and byte range required for phase 1 and intensity thresholds of the phase 3 and 4) of the algorithm can be repeatedly modified in order to improve structures selection. Once the parameters are considered adequate for the whole dataset, the algorithm can be used in batch mode.

## 4. Center-to-limb variation of the fraction of covered surface

The FCS was calculated in each image as the ratio between the number of pixels corresponding to selected structures and the total number of pixels of the image. Resulting values of the FCS are separately presented for the threshold selection criteria and the semi-interactive selection tool. In addition, in each of them, results from March are shown first and September later. Results for the North hemisphere are distinguished in red colour from those for the South in blue. For a better visualization, results from 2007-2011 and 2012-2015 are displayed separately. In all figures, the FCS values are plotted versus $\mu$, i.e., the cosine of the heliocentric angle $\theta$ of the central position of the data.

### 4.1. *Threshold selection criteria*

As described in the work of Cabello *et al.* (2017) and visible in Figs. 1 and 2, the FCS obtained from the intensity threshold selection criteria shows a general decreasing trend from the disk center (values between $\approx 0.005\%$ and $\approx 0.008\%$) to the limb (values $\lesssim 0.002\%$). In both March (Fig. 1) and September (Fig. 2), results corresponding to the northern and southern hemisphere of the lower activity period present similar values at the disk center. However, in the limb, the FCS of the more exposed pole (the South in March and the North in September) has a minimum value around $\mu \approx 0.4$-$0.5$ and a slight increase towards higher latitudes. It is noteworthy that this behaviour is not observable for the more active period. In addition, values of FCS are higher and show higher dispersion for the more active period than those of the lower activity period.

### 4.2. *Semi-interactive selection tool*

Results of FCS obtained from the semi-interactive tool (Figs. 3 and 4) also show a general decrease from solar center to limb, although the decrease is not so steep as with the results from the threshold selection criteria. In this way, values from the center to the limb are from $\approx 0.002\%$ to $\approx 0.001\%$ in the lower activity period and from $\approx 0.003$-$0.004\%$ to $\approx 0.001\%$ in the more active period. However, a minimun and a slighter increase around $\mu \approx 0.4$ can also be observed for the period of the lower activity in the values corresponding to the more exposed pole, i.e. the South in March (Fig. 3) and the North in September (Fig. 4).

The low values obtained at the solar center with the semi-interactive tool are due to the restrictions imposed with the input parameters to avoid selecting features that are

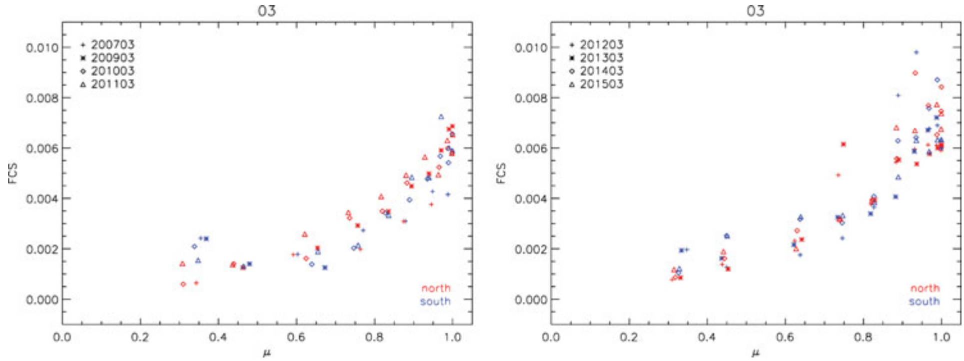


**Figure 1.** CLV of the FCS of small magnetic structures selected with the threshold selection criteria along the central meridian in the North (blue) and South (red) hemispheres on March. Left panel correspond to the more quiet period (2007-2011) and right panel to the more active period (2012-2015).

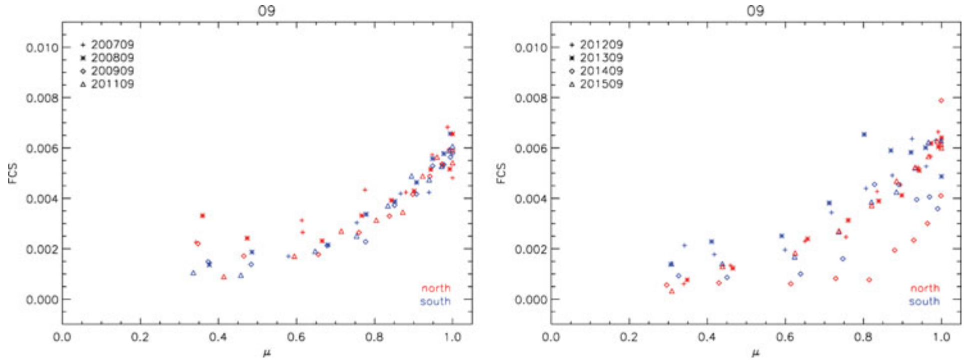


**Figure 2.** Same as Fig. 1, but refering to September.

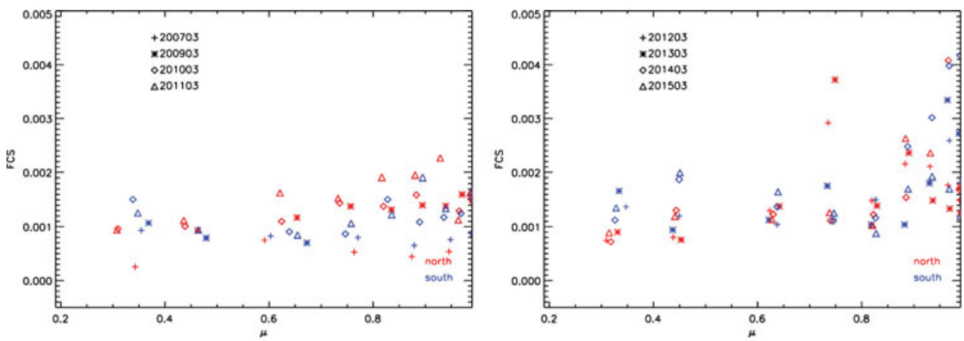


**Figure 3.** Same as Fig. 1, but with the semi-interactive selection tool.

not the desired structures. This inconvenient is not as severe at the limb due to higher intensity contrast values and sizes involved. Work is being done to improve the selection via analysis of sub-fields of each image rather than the full field of view, so the algorithm works locally without disturbances from the whole image.

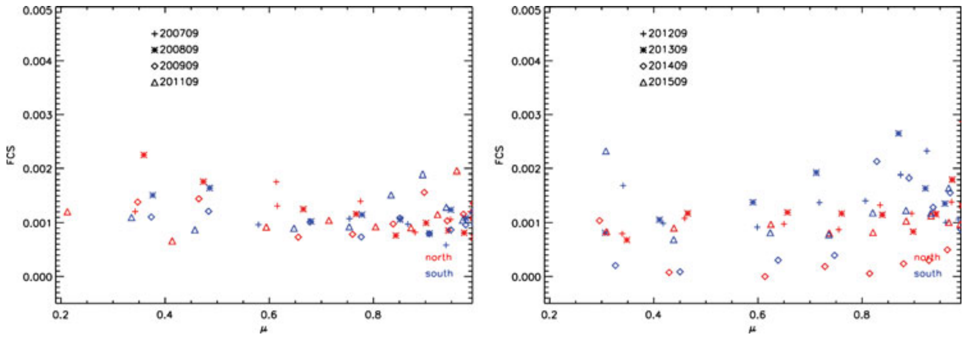


**Figure 4.** Same as Fig. 3, but refering to September.

## 5. Conclusions

The CLV of the FCS of small magnetic structures has been analysed with the results obtained from two different selection techniques: an intensity threshold criteria and a semi-interactive tool. Results obtained from both techniques show a decrease from the center to the limb in both the lower activity and the more active period. However, in the lower activity period a minimum around $\mu \approx 0.4$ and a slight increase towards higher latitudes can be observed in the more exposed hemisphere, i.e. the southern in March and the northern in September. Although currently work is being done to improve the structure selection, in particular with the semi-interactive tool, this analysis suggests an increase of small magnetic structures close to the poles with regard to the rest of the disk in the low activity period. This behaviour is known for other structures like polar faculae and points to the relation of these structures to the global magnetic field, since the latter has a poloidal distribution around minimums of solar cycle.

### Acknowledgement

IC is member of the Carrera del Investigador Científico of CONICET. This work has been partially funded by the Spanish Ministerio de Economía y Competitividad, through Projects ESP2014-56169-C6-4-R and ESP2013-47349-C6-5-R, including a percentage from European FEDER funds. IC is grateful to the project ESP2014-56169-C6-4-R, the IAU and Facultad de Ciencias Exactas y Naturales (UNCuyo) for financial support to attend the Symposium. Hinode is a Japanese mission developed and launched by ISAS/JAXA, with NAOJ as domestic partner and NASA and STFC (UK) as international partners. It is operated by these agencies in co-operation with ESA and NSC (Norway).

### References

Berger, T. E. & Title, A. M. 2001, *ApJ*, 553, 449

Blanco Rodríguez, J., Okunev, O. V., Puschmann, K. G., Kneer, F., & Sánchez-Andrade Nuño, B. 2007, *A&A*, 474, 251

Bonet, J. A., Cabello, I., & Sánchez Almeida, J. 2012, *A&A*, 539, A6

Bovelet, B. & Wiehr, E. 2007, *Solar Phys.*, 243, 121

Cabello, I., Blanco Rodríguez, J., Balmaceda, L., & Domingo, V. 2017, *Boletín de la Asociación Argentina de Astronomía* (sended)

Domingo, V., Ortiz, A., Sanahuja, B., & Cabello, I. 2005, *Adv. Sp. Res.*, 35, 345

Kosugi, T., Matsuzaki, K., Sakao, T., Shimizu, T., Sone, Y.and Tachikawa, S., Hashimoto, T., Minesugi, K., Ohnishi, A., Yamada, T., Tsuneta, S., Hara, H., Ichimoto, K., Suematsu, Y., Shimojo, M., Watanabe, T., Shimada, S., Davis, J. M., Hill, L. D., Owens, J. K., Title, A. M., Culhane, J. L., Harra, L. K., Doschek, G. A., & Golub, L. 2007, *Solar Phys.*, 243, 3

Sánchez Almeida, J., Bonet, J. A., Viticchié, B., & Del Moro, D. 2010, *ApJ*, 715, L26